Novel Synthesis of Tin Dioxide Nanoribbons via a Mild Solution Approach

Changhui Ye,* Xiaosheng Fang, Yinhai Wang, Ting Xie, Aiwu Zhao, and Lide Zhang
Laboratory of Functional Nanomaterials and Nanostructures, Institute of Solid State Physics, Chinese Academy of Sciences, P. O. Box 1129, Hefei 230031, P. R. China

(Received October 20, 2003; CL-030980)

Single crystalline tin dioxide nanoribbons have been synthesized in bulk quantity by a mild solution approach using cetyltrimethylammonium bromide surfactant as a soft template. The as-synthesized SnO_2 nanoribbons have a length up to tens of micrometers, width of several hundred nanometers, and thickness of several tens of nanometers.

Tin dioxide, an important wide bandgap semiconductor, has been used as effective gas sensors,[1] transparent conducting electrodes,[2] and dye-based solar cells.[3] Low-dimensional SnO_2 nanomaterials, such as nanowires, nanorods, and nanoribbons can be expected to exhibit special optical and electrical properties. Recently, nanoribbons or nanobelts of SnO_2 have been synthesized by chemical vapor deposition (CVD) methods in many groups,[4–12] and the ribbon-like nanostructures have been expected to represent important building blocks for nanodevices and offer exciting opportunities for both fundamental research and technological application. For example, Yang et al. have demonstrated that SnO_2 nanoribbons are excellent gas sensors for nitrogen dioxide.[13] However, high temperature (800 °C or higher) was needed for these groups to synthesize SnO_2 nanoribbons and complicated experimental setups were generally required.

In this letter, we introduce a novel solution approach to synthesize nanoribbons of the semiconductor SnO_2. In a typical synthesis, cetyltrimethylammonium bromide (CTAB; 1.093 g) was added to a 0.015 M $SnCl_2$ solution (80 mL), and NaOH solution was added to bring the pH value of this solution to 14, with vigorous stirring for 2 h to ensure the complete dissolution of CTAB and sufficient attachment of $HSnO_2^-$ on head groups of CTAB. To the solution 1.0 mL of H_2O_2 was added. After the solution was stirred at room temperature overnight, it was maintained at 60 °C for 4 h, and then the resulting pale white products (SnO_2) were collected, washed several times using absolute ethanol and distilled water, and dried at room temperature.

For the synthesis of SnO_2 nanoribbons, the redox reaction at basic condition can be shown as follows:

$$HSnO_2^- + HO_2^- \rightarrow SnO_2 + 2OH^-$$

The standard Gibbs free energy change $\Delta_r G_m^\circ$ of the redox reaction was calculated to be $-119.5\,kJ\cdot mol^{-1}$ on the basis of standard reduction potential values, which implied a very strong tendency for the reaction to proceed toward the products. X-ray powder diffraction (XRD) pattern of the sample is shown in Figure 1, where all diffraction peaks can be indexed to the tetragonal SnO_2 (space group: $P4_{2/mnm}$) with lattice constants $a = 0.4734$ nm and $c = 0.3180$ nm (JCPDS 41-1445). The XRD pattern indicates that the nanoribbons obtained via our current synthetic approach consist of pure phase of tetragonal SnO_2, and there is no other phase of SnO_2 or any phase of SnO in the products. Though the crystalline quality might not be perfect, the SnO_2 nanoribbons are stable under the intense electron illumination in a microscope.

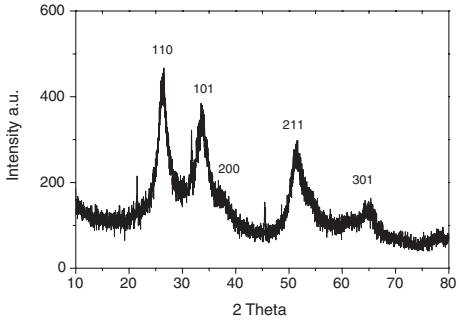

Figure 1. XRD pattern of the SnO_2 nanoribbons. All the diffraction peaks can be readily indexed to tetragonal phase SnO_2.

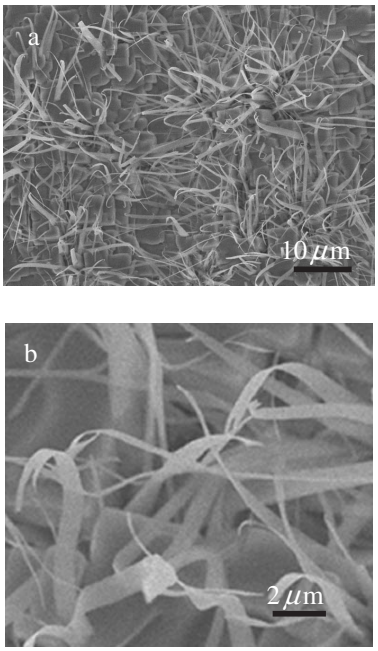

Figure 2. SEM images of the SnO_2 nanoribbons. (a) and (b) are low magnification and high magnification views, respectively.

The morphology of the as-synthesized SnO_2 nanoribbons was studied with scanning electron microscopy (SEM). Typical SEM images (Figure 2) showed that the sample consists of SnO_2 nanoribbons and nanoplatelets. The nanoribbons are typically tens of nanometers to near 1 μm in width and up to tens of micrometers in length, with their thickness being very small. A representative transmission electron microscopy (TEM) image of a 1 μm wide SnO_2 nanoribbon is displayed in Figure 3a. The bend-

ing contours are clearly observed and typical for nanoribbons. Figure 3b exhibits a high-resolution electron microscopy (HREM) image of the nanoribbon. The spacing of 0.471 nm between two lattice planes corresponds to the separation between (010) planes of tetragonal SnO_2. The selected-area electron diffraction (SAED) pattern taken along $\langle 10\bar{2} \rangle$ zone axis in the inset shows that the growth direction of the nanoribbon is along [101]. The nanoribbons are bound by pairs of $(10\bar{1})$ top, (010) edge and (201) end surface planes. On the basis of the HREM image and the SAED pattern, the SnO_2 nanoribbons in the present study are determined to be single crystalline. What worth mentioning is that the production of SnO_2 nanomaterials by the present method is very effective and more than 90% of the precursor can be transformed to the final product. However, relatively pure SnO_2 nanoribbons could only be obtained above a moderately high CTAB concentration.

Surfactants have been frequently used to direct or template the growth of a wide variety of nanostructures.[14–18] When reaching a critical concentration, surfactants will form various structures known as micelles.[19] Layered structure is also well-documented for many surfactants and is displayed schematically in Figure 4. After this structure formed, and $HSnO_2^-$ sufficiently adsorbed on the surface near the head part of the CTAB micelles, upon the oxidation by H_2O_2, SnO_2 would nucleate and eventually, single crystalline SnO_2 nanoribbons were obtained after stirring and heat treatment processes. However, as reported in the literature[19] and noted in the present study, the concentration of the surfactant and the ionic strength of the solution played a significant role in the formation of various micellar structures. We also found out that changing these experimental parameters could lead to morphology transformation of the nanostructure, including nanoparticles, nanowires, and nanoribbons. Further work is underway to clarify the structural evolvement processes.

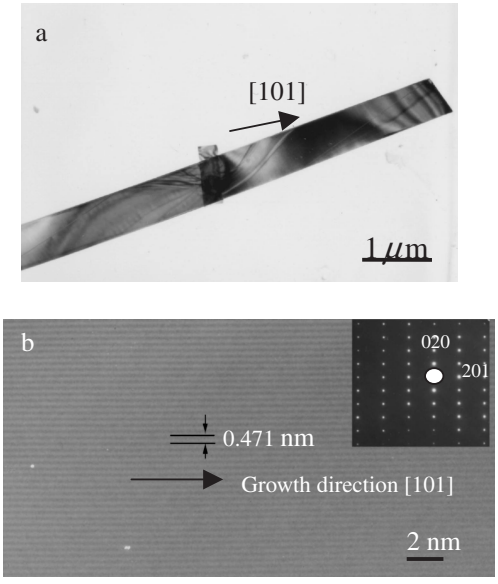

Figure 3. (a) and (b) TEM and HREM images of a SnO_2 nanoribbon, respectively. Inset in (b) is the corresponding SAED pattern taken along $\langle 10\bar{2} \rangle$ zone axis.

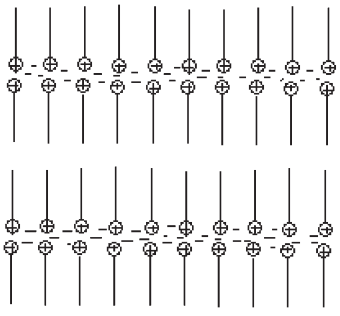

Figure 4. Schematic illustration of layered structure of a surfactant micelle. ⊕ denotes positively charged head group of the surfactant CTAB molecules, $(CH_3)_3N^+$ here; — denotes the tail of the surfactant CTAB molecules, $CH_3(CH_2)_{15}$ here; – near the head of the micelle denotes negatively charged $HSnO_2^-$ ions.

In summary, we have obtained single crystalline SnO_2 nanoribbons by a novel, mild solution route. The control of concentration of the surfactant CTAB is the critical factor for obtaining large quantity of single crystalline SnO_2 nanoribbons. Our method is facile, less costly and reproducible. We believe that this novel approach can be extended to preparation of a wide variety of other oxide nanoribbons.

Financial supports from Anhui Provincial Natural Science Foundation (Grant number 03044905) and National Science Foundation of China (Grant number 10304018) are gratefully acknowledged.

References

1 A. Dieguez, A. R. Rodriguez, J. R. Morante, U. Weimar, M. S. Berberich, and W. Gopel, *Sens. Actuators*, **31**, 1 (1996).
2 Y. S. He, J. C. Campbell, R. C. Murphy, M. F. Arendt, and J. S. Swinnea, *J. Mater. Res.*, **8**, 3131 (1993).
3 S. Ferrere, A. Zaban, and B. A. Gregg, *J. Phys. Chem. B*, **101**, 4490 (1997).
4 Z. R. Dai, Z. W. Pan, and Z. L. Wang, *Solid State Commun.*, **118**, 351 (2001).
5 Z. W. Pan, Z. R. Dai, and Z. L. Wang, *Science*, **291**, 1947 (2001).
6 X. H. Kong, D. P. Yu, and Y. D. Li, *Chem. Lett.*, **32**, 100 (2003).
7 X. S. Peng, L. D. Zhang, G. W. Meng, Y. T. Tian, Y. Lin, B. Y. Geng, and S. H. Sun, *J. Appl. Phys.*, **93**, 1760 (2003).
8 J. Q. Hu, Y. Bando, and D. Golberg, *Chem. Phys. Lett.*, **372**, 75870 (2003).
9 S. H. Sun, G. W. Meng, Y. W. Wang, T. Gao, M. G. Zhang, Y. T. Tian, X. S. Peng, and L. D. Zhang, *Appl. Phys. A*, **76**, 287 (2003).
10 J. Q. Hu, Y. Bando, Q. L. Liu, and D. Golberg, *Adv. Funct. Mater.*, **13**, 493 (2003).
11 J. Q. Hu, X. L. Ma, N. G. Shang, Z. Y. Xie, N. B. Wong, C. S. Lee, and S. T. Lee, *J. Phys. Chem. B*, **106**, 3823 (2002).
12 J. K. Jian, X. L. Chen, W. J. Wang, L. Dai, and X. P. Xu, *Appl. Phys. A*, **76**, 291 (2003).
13 M. Law, H. Kind, B. Messer, F. Kim, and P. Yang, *Angew. Chem., Int. Ed.*, **41**, 2405 (2002).
14 W. Z. Wang, Y. J. Zhan, and G. H. Wang, *Chem. Commun.*, **2001**, 727.
15 N. R. Jana, L. Gearheart, and C. J. Murphy, *Adv. Mater.*, **13**, 1389 (2001).
16 C. N. R. Rao, A. Govindaraj, F. L. Deepak, and N. A. Gunari, *Appl. Phys. Lett.*, **78**, 1853 (2001).
17 E. Leontidis, T. K. Leodidou, W. Caseri, and K. Kyriacou, *Langmuir*, **15**, 3381 (1999).
18 L. Wang, S. Tomura, F. Ohashi, M. Maeda, M. Suzuki, and K. Inukai, *J. Mater. Chem.*, **11**, 1464 (2001).
19 B. Y. Zhu and Z. G. Zhao, "Introduction to Interface Chemistry," Chemical Industry Press, Beijing (1996).

Published on the web (Advance View) December 15, 2003; DOI 10.1246/cl.2004.54